Prioritizing hotspots for Carbon Capture and Storage Deployment in China's Cement Sector: A County-level Analysis

Tongyuan Wu[1], Thomas S.T. Ng[2,*], Ji Chen[3], Yihan Wang[4]

1 = Department of Architecture and Civil Engineering, City University of Hong Kong, Hong Kong, China. Email address: wty20@connect.hku.hk.
2 = Department of Architecture and Civil Engineering, City University of Hong Kong, Hong Kong, China. Email address: thomasng@cityu.edu.hk.
3 = Department of Civil Engineering, The University of Hong Kong, Hong Kong, China. Email address: jichen@hku.hk.
4 = Department of Civil Engineering, The University of Hong Kong, Hong Kong, China. Email address: wangyh22@hku.hk.
* = corresponding author.

Abstract:

Carbon capture and storage (CCS) is essential for decarbonizing the hard-to-abate cement sector, but its large-scale deployment must strategically align with spatial storage availability to maximize feasibility and efficiency. However, the impacts of future demand and supply layouts on CCS deployment remain unexplored, limiting the understanding of optimal locations for implementation. This study identifies priority counties for CCS deployment in China's cement sector by integrating projected national cement demand by 2050 with three spatial allocation scenarios—population-driven (POP), GDP-driven (GDP), and a POP-GDP hybrid scenario—to estimate county-level clinker production and associated carbon emissions. These emissions are then matched with available carbon storage capacities from deep saline aquifers (DSA) and CO_2-enhanced oil recovery (EOR) sites, while minimizing transportation distances. The results reveal significant spatial mismatches: eastern and southern high-emission production hubs often lack nearby storage capacity, whereas western and northern counties possess ample storage but lower emissions. Optimized emissions-storage matching highlights that counties in Yunnan, Guizhou, and Xinjiang offer greater feasibility for CCS due to shorter transportation distances and sufficient storage capacity. These findings underscore the importance of integrating cement production planning with CCS infrastructure development to enhance mitigation efforts, reduce transportation costs, and improve sequestration efficiency, supporting the transition toward a net-zero cement industry.

Keywords: cement sector; clinker production; spatial analysis; carbon capture and storage (CCS); county-level

Graphical abstract:

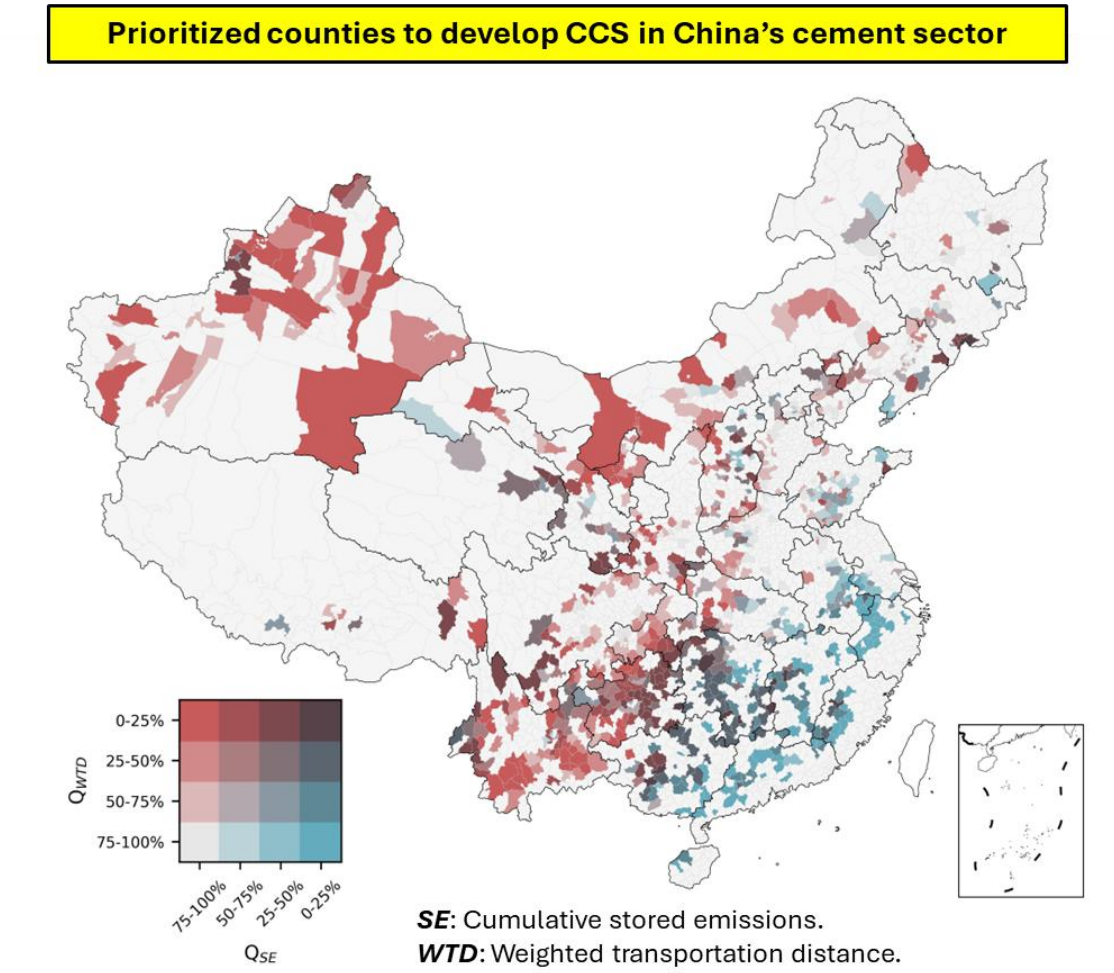

1. Introduction

China's cement sector produces over two billion tons of cement per year (National Bureau of Statistics of China, 2021), resulting in approximately 1.3 gigatons (Gt) of CO_2 emissions (Wu et al., 2022). These substantial emissions are challenging to abate, because they include inherent 'process' emissions released by the decomposition of limestone during calcination, which cannot be fully mitigated only through conventional measures such as thermal efficiency improvements and low-carbon fuels (Habert et al., 2020). Furthermore, alternative types of cement and clinker are still unready for large-scale deployment (Gartner and Sui, 2018). Therefore, carbon capture and storage (CCS) still plays a key role in the net-zero transition for the cement sector (Fennell et al., 2021), despite its high cost and limited technological readiness (Gardarsdottir et al., 2019; Voldsund et al., 2019).

Previous studies have investigated the contribution of CCS to the net-zero transition from a supply-side perspective (Dinga and Wen, 2022; Ren et al., 2023; Tan et al., 2022; Yu Wang et al., 2023; Zhang et al., 2021). For instance, Tan et al. (2022) revealed that at least 50% of production capacity should be equipped with CCS by 2060, leading to a 28% reduction in CO_2 emissions. Ren et al. (2023) showed that energy-efficient technologies are crucial for mitigating near-term CO_2 emissions, but in the long term, achieving net-zero emissions requires large-scale implementation of CCS combined with bioenergy. Furthermore, some pilot efforts have demonstrated the shrinking role of CCS if material efficiency strategies are implemented to mitigate future cement production from the demand side (Watari et al., 2022; Wu et al., 2023). Watari et al. (2022) found that implementing demand-side strategies at just 50% of their technical potential could reduce the requirement for cement kilns with CCS from 70% to 30%, enabling a net-zero cement sector in Japan by 2050. Wu et al. (2023) showed that more intensive use and extending lifetime of in-use cement stock can significantly reduce future demand, potentially achieving a net-zero cement sector with a moderate combination of supply-side measures, even with limited CCS deployment.

Furthermore, the extent to which the above delineated potentials of CCS can be tapped, hinges on the effective matching of emissions sources with accessible storage sites (Gibbins & Chalmers, 2008; IEA, 2016). Without considering spatial factors including proximity, capacity, and infrastructure availability, the scaling up of CCS technologies may face significant logistical and economic challenges, particularly in regions with uneven distribution of emissions and storage resources (IEA, 2019). As such, Wei et al. (2021) cost-effectively matched 3,093 carbon clusters with 432 sinks to develop a global layout of carbon capture, utilization and storage (CCUS), achieving a cumulative mitigation of 92 Gt CO_2. Tang et al. (2023) proposed a spatial CCUS network of emissions sources, sinks, and transportation pipelines for multiple industrial sectors in China to achieve carbon neutrality. Recently, Wang et al. (2024b) proposed optimal layouts of cement plants for CCS deployment under different national mitigation targets, with particular attention to the increased energy and water consumption required to support CCS facilities.

However, there is a lack of consideration for the impact of changing spatial demand layouts, on the emissions mitigation efforts, especially for CCS deployment. Whilst previous spatial analyses have been conducted to characterize emissions dynamics and drivers at the province level (Liu et al., 2021, 2018; Zhang et al., 2015), a few studies have tried to investigate more refined spatial levels, such as city level (Yihan Wang et al., 2023), county level (Xu et al., 2024), or even plant level (Wang et al., 2024a). For instance, Yihan Wang et al. (2023) explicitly evaluated the eco-efficiency of cement sector for each city in China to identify areas with concentrated high energy consumption and CO_2 emissions. Compared to province-level analysis, these insights could reveal greater regional heterogeneity in emissions dynamics, helping to identify priority regions for future mitigation efforts. Given this, Xu et al. (2024) projected future county-level cement production and related CO_2 and air pollutant emissions using an artificial neural network model based on multiple spatially refined features. Moreover, Wang et al. (2024a) decomposed industry-level green transformation pathways for cement plants in China, not only to improve feasibility but also to identify priority units for retrofitting or retirement in the near term. Nevertheless, the impacts of changing demand layouts have seldom been considered in previous studies.

As such, identifying optimal locations for CCS deployment can reduce transportation costs, enhance efficiency, and ensure that storage capacities are not exceeded (Middleton and Bielicki, 2009). Nevertheless, previous decarbonization roadmaps for cement sector lack spatially explicit guidance for practical implementation (Dinga and Wen, 2022; Ren et al., 2023; Tan et al., 2022; Zhang et al., 2021). Especially for CCS deployment, it is essential to consider suitable capacities for retrofitting as well as local or nearby accessible storage sites for captured emissions. Implicit spatial information or overlooking regional discrepancies may hinder the scaling up of CCS in the cement sector. Additionally, whilst some source-sink matching analyses have been conducted for CCS deployment in energy and industrial sectors (Tang et al., 2021; Wang et al., 2024b; Wei et al., 2021), the impacts of changing emissions layouts caused by future demand are seldom investigated, which may pose the risks of stranded assets of these capital-intensive facilities and infrastructures.

This study addresses the above gap by conducting a spatial supply-demand and emissions-storage matching analysis for CCS deployment in cement sector across China's counties. This study starts with allocating future national cement clinker demand to individual counties and simulating clinker production capacity turnover. It then performs county-level supply-demand matching, estimates carbon storage potentials, and matches emissions to storage sites. Finally, strategic locations can be identified for large-scale CCS deployments, providing spatially explicit insights into the feasibility and optimization of CCS in China's cement sector.

2. Methods

This study takes China's counties as a demonstration case to conduct spatial analysis, providing clear, spatially explicit insights into priorities for CCS deployments in the cement sector. The research framework consists of six interlinked modules (Figure 1). First, national cement demand is projected to 2050 under the socio-economic drivers (Module 1, Section 2.1). Second, this

projected demand is spatially downscaled to the counties, based on three allocation schemes (Module 2, Section 2.2). Third, the resulting county-level demand is matched with nearby supply capacity while minimizing transport distances, to determine annual production of each county (Module 3, Section 2.3). In parallel, Module 4 (Section 2.4) dynamically simulates the evolution of production capacity and continuously feeds updated capacity information back into Module 3 for demand matching. Fifth, both carbon emissions from cement clinker production and carbon storage capacities are estimated at the county level (Module 5, Section 2.5). Finally, the cumulative emissions are spatially matched and planned to be stored in the available capacities nearby, while minimizing total transportation distances (Module 6, Section 2.6). Counties with substantial emission and considerable nearby storage capacity are identified as priorities for future CCS development in China's cement sector. To evaluate the robustness of model assumptions, we conduct a scenario-based sensitivity analysis on key parameters, including cement demand projections, kiln turnover rules, and carbon storage capacities (see Supplementary Information S3).

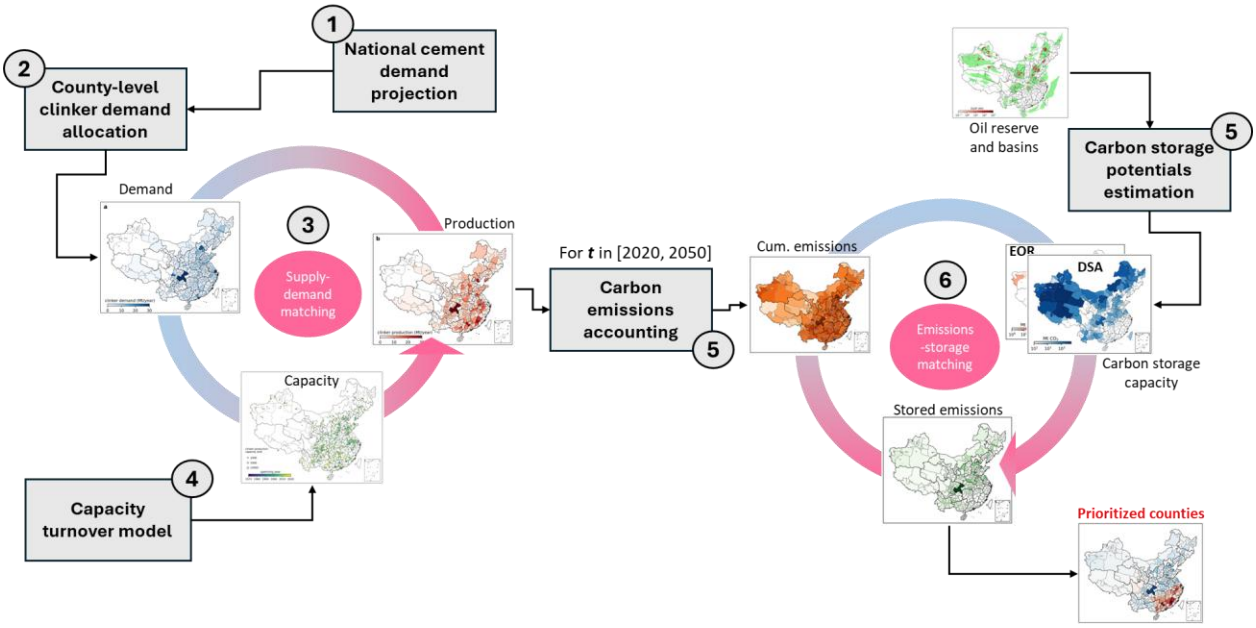

Figure 1 | Overview of the research framework. Notes: The number 1-6 in the ovals represents the six modules in the following sub-sections.

2.1 Projecting future national cement demand

We adopted and slightly modified the method proposed by Van Ruijven et al. (2016) to estimate future cement demand. This method captures the S-shaped relationship between per-capita consumption and GDP through a non-linear model. In this study, we used a Gaussian-like function to fit the historical trend. As for future, per-capita consumption (pcc_t) is extrapolated based on an exponential decay of the deviation (Δ) between the current per-capita consumption (pcc_{t_0}) and the future saturated level ($pcc_{saturated}$).

$$pcc_t = a \times e^{-\left(\frac{pGDP_t - b}{c}\right)^2} \quad (t \leq 2020) \tag{1}$$

$$pcc_t = pcc_{saturated} + \Delta \times e^{-\gamma \times (pGDP_t - pGDP_{t_0})} \quad (t > 2020) \tag{2}$$

where γ controls the speed of the decay. The national cement demand (C_t) is then calculated by multiplying the projected per-capita consumption by the future population (P_t).

$$C_t = pcc_t \times P_t \tag{3}$$

2.2 Downscaling national demand to county level

After projecting the national cement demand, we downscaled it to the county level based on three different assumptions. First, national demand was allocated to the counties according to the future population distribution, which implies that all counties would have the same cement demand per capita. Second, national demand was allocated to the counties based on future GDP distribution, which implies that the counties will have the same cement demand relative to their GDP. Third, the allocation took both population and economic factors into account. Therefore, the county-level demand was calculated as below.

$$c_{i,t} = w_{i,t} \times C_t \tag{4}$$

$$w_{i,t} = \frac{\beta \times p_{i,t} + (1 - \beta) \times g_{i,t}}{\sum_i [\beta \times p_{i,t} + (1 - \beta) \times g_{i,t}]} \tag{5}$$

where $w_{i,t}$ represents the weight for allocating national demand to a specific county i in year t. The coefficient β is used to balance the impact of population and GDP in the allocation process. Here, $p_{i,t}$ and $g_{i,t}$ are the proportions of population and gross domestic product (GDP) in county i relative to the national total. Thus, the three scenarios based on the above assumptions are summarized in Table 1, which help address the uncertainty in socio-economic drivers. And the county-level cement demand would be converted to clinker demand according to future clinker-to-cement ratio (CCR) in Table S1.

Table 1 | Demand allocation scenarios and related assumptions.

Scenario	Assumption
POP	Future cement demand will be allocated based on population distribution (i.e., $\beta = 1$).
GDP	Future cement demand will be allocated based on economic output distribution (i.e., $\beta = 0$).
POP-GDP	Future cement demand will be allocated based on both population and economic output distribution (i.e., $\beta = 0.5$).

2.3 Matching county-level demand and supply

After allocating the county-level demand, we optimized the nationwide clinker production layout at the county level by matching each county's demand with the available supply capacity nearby, with the objective of minimizing the total transportation cost. This cost is calculated as the sum of shipping distances weighted by the amount of supply transported (TC_t). Here, we assumed a uniform shipping cost across counties. The optimization model can be formulated as follows:

$$\min TC_t = \sum_{i=1}^{N}\sum_{j=1}^{N} d_{i,j} \times x_{i,j,t} \tag{6}$$

where the decision variable $x_{i,j,t}$ denotes the amount of supply transported from county i to county j in year t, and $d_{i,j}$ is the shortest driving distance between the centroids of county i and county j. The optimization is subjective to two main constraints. First, the total supply from each county must not exceed its available production capacity ($S_{i,t}$). Second, the total supply received by each county must meet its demand ($c_{j,t}$). Additionally, all shipment amounts must be non-negative.

$$\sum_{j=1}^{N} x_{i,j,t} \leq S_{i,t} \tag{7}$$

$$\sum_{i=1}^{N} x_{i,j,t} = c_{j,t} \tag{8}$$

$$x_{i,j,t} \geq 0 \tag{9}$$

Thus, optimization ensures that the supply from each county is efficiently allocated to meet the demand while minimizing the total transportation cost. This approach allows for a cost-effective solution to match supply and demand at the county level, considering both logistical constraints and geographical distances. We solved this linear optimization model in Python using the Gurobi Optimizer (Gurobi Optimization, LLC, 2025) via the Gurobipy interface, to determine the optimal production layout.

2.4 Modeling turnover of production capacity

We adopted and improved upon the method proposed in our previous work (Wu et al., 2025) to simulate the turnover process of production capacity for each county in the future. Specifically, cement kilns would either operate to produce clinker, retire, or shut down based on various conditions. The turnover process for each county can be described by four distinct sets of kilns, as outlined below:

$$K_{i,t}^{retired} = \left\{ k^{t_1} \in K_{i,t-1}^{operating} \middle| t_1 - t > L \right\} \tag{10}$$

$$K_{i,t}^{shutdown} = \left\{ k^{t_1} \in K_{i,t-1}^{operating} \middle| \left(t_1 - t > \frac{L}{2} \right) \& (u_{t-1} < 0.3) \right\} \quad (11)$$

$$K_{i,t}^{new} = \{ k_1^t, k_2^t, \ldots, k_n^t \} \quad (12)$$

$$K_{i,t}^{operating} = \left(K_{i,t-1}^{operating} \backslash K_{i,t}^{retired} \right) \cup K_{i,t}^{new} \quad (13)$$

where $K_{i,t}^{operating}$, $K_{i,t}^{retired}$, $K_{i,t}^{shutdown}$, and $K_{i,t}^{new}$ represent the sets of operating, retired, shutdown, and new cement kilns in county i at year t, respectively. Here, k^{t_1} denotes the annual production capacity of a cement kiln that began operation in year t_1, and L represents the expected lifespan of a cement kiln (40 years). The underutilized capacity will gradually shut down to address over-capacity issues if its utilization rate (u) falls below 30% and the cumulative operation period exceeds half of the expected lifespan. The new capacity will be developed to address the future emerging gaps between supply and demand.

2.5 Estimating carbon emissions and storage capacity

2.5.1 Carbon emissions from clinker production

The carbon emissions from cement clinker production in county i during year t can be estimated by multiplying the annual clinker output ($O_{i,t}$) by the emission intensity of clinker production ($e_{i,t}$).

$$E_{i,t} = O_{i,t} \times e_{i,t} \quad (14)$$

The emission intensity is determined by a series of factors, including future thermal energy intensity, the share of alternative fuels, electricity usage, the emission factors of power generation, and the clinker-to-cement ratio (see Table S1 for details).

2.5.2 Carbon storage capacity

Whilst CO_2 can be sequestered in oil and gas reservoirs, sedimentary basins for aquifer storage, and unmineable coal areas (Szulczewski et al., 2012), only deep saline formations and CO_2-EOR (enhanced oil recovery) in oil reserves are considered in this study, primarily due to the safety concerns about geological storage (Lackey et al., 2019). This study adopted the methodologies synthesized by Wei et al., (2021) to estimate carbon storage potentials of oil and gas field (G_{EOR}) and saline aquifer basins (G_{DSA}). The former is estimated by multiplying the quantity of enhanced oil recovery (EOR) with the typical ratio of required CO_2 injection to unit oil recovered (R_{CO_2}), which depends on the oil formation depth and API (i.e., American Petroleum Institute) gravity:

$$G_{\mathrm{EOR}} = EOR \cdot R_{CO_2} \quad (15)$$

And the amount of enhanced oil recovery is calculated as:

$$EOR = \left(\frac{OOIP}{\rho_{\text{oil}}}\right) \cdot B_o \cdot \tau_{\text{EOR}} \cdot EXTRA \tag{16}$$

where $OOIP$ denotes the original oil-in-place, of which the data are retrieved from *2000 World Petroleum Assessment* (Persits et al., 2000). ρ_{oil} is the density of crude oil. B_o is the oil formation volume factor, which converts the volume of oil at standard conditions to that at reservoir pressure and temperature; and τ_{EOR} is a "contact" factor, representing the proportion of $OOIP$ that comes in contact with the CO_2 injected into the formation, which directly influences the carbon storage efficiency. $EXTRA$ represents the proportion of extra recovery to the $OOIP$ contacted with CO_2, represented as a percentage. This factor depends on the API gravity of crude oil. As for deep saline aquifers (DSA), the carbon storage potential is estimated as follows.

$$G_{\text{DSA}} = A_{\text{basin}} \times \varphi \times h \times \phi \times \rho_{CO_2-sto} \times \tau_{\text{DSA}} \tag{17}$$

where A_{basin} is the geographical area that defines the basin being assessed for carbon storage. φ denotes the ratio of effective areas for storage. h denotes the gross thickness of saline formations within the basin. ϕ indicates the total porosity in volume defined by the thickness. ρ_{CO_2-sto} denotes the density of CO_2 in storage conditions. again τ_{DSA} denotes a factor for storage efficiency, under the conditions of saline aquifer storage. The values for the above parameters are displayed in Table S2.

2.6 Matching county-level carbon emissions and storage

Finally, this study identified the counties prioritized for developing carbon capture and storage (CCS), by matching the cumulative carbon emissions from clinker production with the available carbon storage capacity within the transportation distance. Specifically, the matching process is expressed as a minimization of the sum of transportation distances weighted by the emissions transported and stored (TS_t):

$$\min TS_t = \sum_{i=1}^{N} \sum_{j=1}^{N} d_{i,j} \times y_{i,j,t} \tag{18}$$

Where $y_{i,j,t}$ is the transported cumulative emissions from county i to county j by year t. The distance $d_{i,j}$ here still represents the shortest driving distance along highways between the centroids of paired counties. This assumes that carbon emissions will be transported either by highway or by pipelines constructed along the existing road infrastructure, carefully avoiding terrain obstacles as much as possible. The optimization model for emissions transportation and storage is subjected to two main constraints. First, the emissions transported from county i to other counties by year t should not exceed the cumulative emissions from clinker production in county i until year t (Equation 19). Second, total emissions transported from other counties to and stored in county j should not exceed its carbon storage capacity G_j, which is available through both

enhanced oil recovery and deep saline aquifers (Equation 20). Additionally, all transportation amounts must be non-negative (Equation 21).

$$\sum_{j=1}^{N} y_{i,j,t} \leq \sum_{m=2021}^{t} E_{i,m} \tag{19}$$

$$\sum_{i=1}^{N} y_{i,j,t} \leq G_j \tag{20}$$

$$y_{i,j,t} \geq 0 \tag{21}$$

Again, we solved this linear optimization model in Python using the Gurobi Optimizer (Gurobi Optimization, LLC, 2025) via the Gurobipy interface, to determine the optimal emission transportation and storage layout. After matching emissions and storage capacities, we would calculate the transportation distance weighed by stored emissions ($WTD_{i,t}$) for each county. This indicator can be integrated with the total stored emissions to identify the counties which have both substantial stored emissions and acceptable transportation distances.

$$WTD_{i,t} = \frac{\sum_{j=1}^{N} d_{i,j} \times y_{i,j,t}}{\sum_{j=1}^{N} y_{i,j,t}} \tag{22}$$

Furthermore, by considering different future cement demand scenarios, our methodology ensures robust identification of counties where CCS can be most effective. It optimizes transportation distances and storage capacities, targeting areas with high emissions and accessible storage sites, thereby maximizing the efficiency of carbon capture and storage.

2.7 Data source

This study retrieved data on national cement production, imports, and exports from the *National Data* platform (National Bureau of Statistics of China, 2025), to fit the historical trend and project future demand. Then for demand downscaling, we adopted the SSP2 "middle-of-the-road" from the gridded dataset of future population[1] (Wang et al., 2022) and GDP[2] (Wang and Sun, 2022), and aggregated them to the county-level. For matching supply and demand, this study computed the shortest highway driving distances between the centroids of paired counties by the route planning function on Amap's application programming interface[3]. For emissions accounting, the parameters

[1] https://doi.org/10.6084/m9.figshare.19608594.v3
[2] https://zenodo.org/records/7898409
[3] Website: https://lbs.amap.com/.

to estimate the future emission intensity of clinker production are determined based on our previous work on China's cement sector (Wu et al., 2025, 2023, 2022). Finally, to assess carbon storage capacity, we collected the locations and area of basins and deep saline aquifers in China are retrieved from the maps of *Geologic Provinces of the Far East, 2000 (prv3al)* developed by United States Geological Survey (1999), whereas the locations and reserve of oil fields are retrieved from the *Atlas of China's Petroliferous Basins* compiled by Li & Lv (2002) (see Figure S1 for details).

3. Results and discussion

3.1 Future county-level cement demand in China

Figure 2 illustrates the fitted historical trend for national cement demand in China (1990-2024) and the projected cement demand from 2025 to 2050. The prediction demonstrates strong alignment with observed historical patterns, with most errors within ±10% during the recent decades. This suggests that the model is robust in capturing historical demand fluctuations, including the rapid growth phrase (1990-2014) and the post-2015 decline driven by infrastructure saturation and economic transition. Looking ahead, the projection indicates a continuous decline from around 1,900 million tons per year (Mt/year) in 2024 to approximately 800 Mt/year by 2050 – a reduction of 57%. This decline is primarily driven by a combination of decreasing per-capita cement demand alongside future economic growth (Van Ruijven et al., 2016) and the projected downward population trend under the SSP2 scenario.

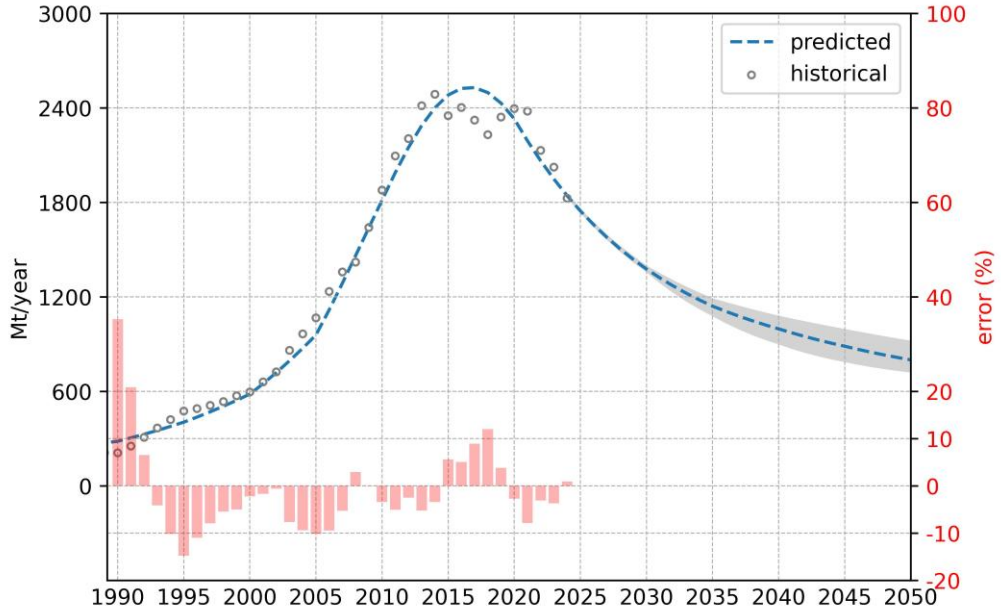

Figure 2 | Predicted future national cement demand in China. Notes: The shaded area around the predicted future cement demand represents the uncertainty range derived from the data of SSP1-5.

Figure 3 displays the future county-level cement demand layout of POP, GDP, and POP-GDP scenarios for 2030, 2040, and 2050, respectively. In the POP scenario, the demand scale varies according to the future population distribution within the counties. Specifically, the demand would be as high as 4-6 Mt/year in Pudong New District of Shanghai and Chaoyang District of Beijing in 2030 (Figure 3a), while it could be as low as a few thousand tons per year in counties with much smaller population, such as Gamba County in Tibet and Hegang County in Heilongjiang. In contrast, under the GDP scenario, cement demand varies significantly across the more developed regions, such as the Beijing-Tianjin-Hebei region, the Yangtze River Delta and the Pearl River Delta (Figure 3b). For instance, cement demand in Chaoyang district of Beijing and Minhang district of Shanghai will increase by approximately 8.3 and 6.2 Mt/year, respectively, compared to the POP scenario. However, the differences across counties would shrink in the POP-GDP scenario (Figure 3c), as it accounts for both the population and economic factors. Overall, these three scenarios provide a broad range of future cement demand across the counties in China.

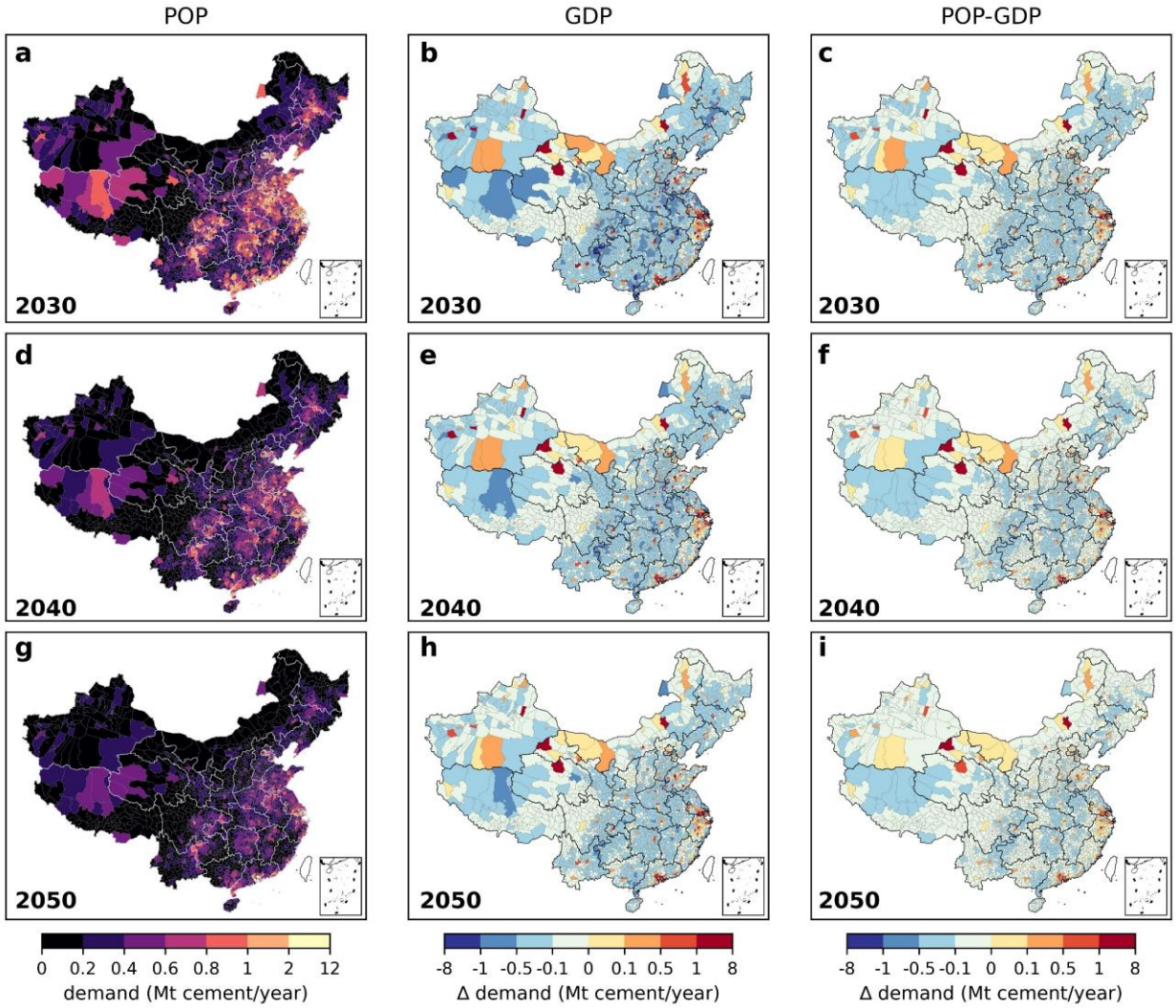

Figure 3 | Future county-level cement demand of POP scenario, and the change in GDP and POP-GDP scenarios compared to POP scenario.

3.2 Existing clinker capacity and production across China

Figure 4a illustrates the distribution of cement clinker production capacity across counties in China in 2020. A total of 814 counties host at least one cement kiln. Among these, about 86% of counties have a clinker production capacity of less than 4 Mt per year, indicating that most counties have relatively minor production capacities. Notably, there are several key production hubs across the country, including the junction of Anhui, Zhejiang, and Jiangsu provinces, northern Guangdong province, and western Fujian province. For instance, Fanchang district of Wuhu city leads with the highest clinker production capacity at 26 Mt per year, followed by Yingde of Qingyuan city with approximately 21 Mt per year, and Liyang of Changzhou city with around 20 Mt per year. In contrast, Huanren of Benxi city in Liaoning province has the smallest clinker production capacity, at just 13 Kt per year.

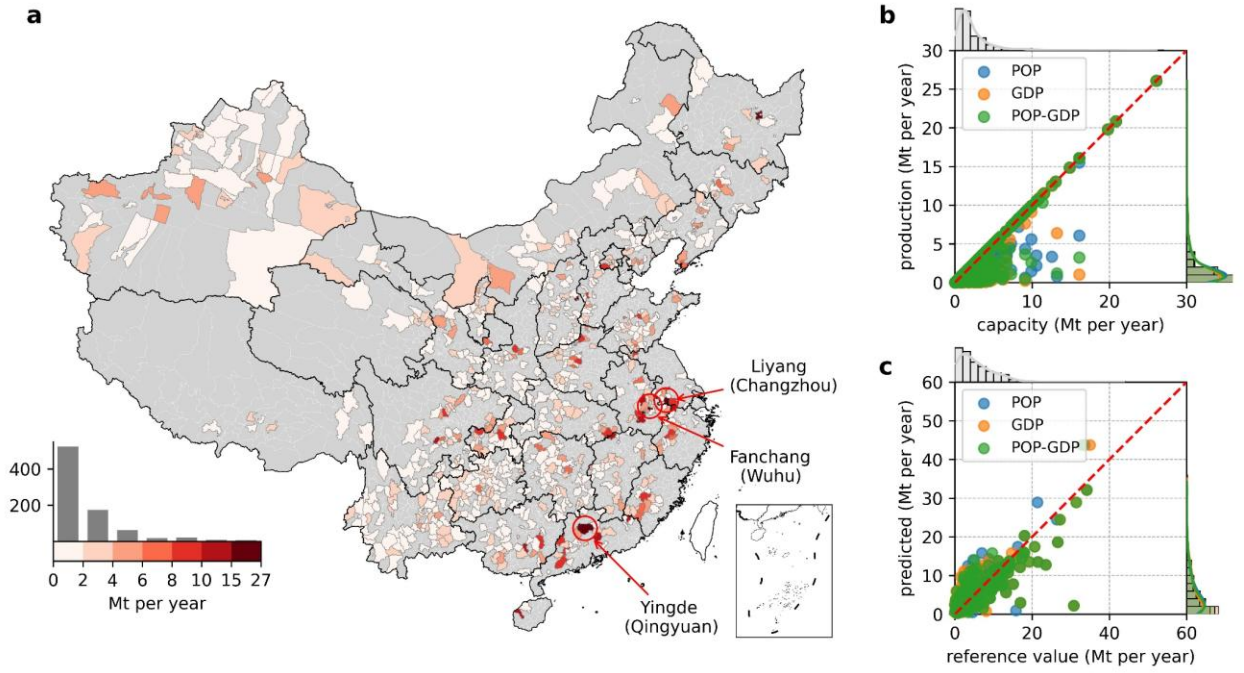

Figure 4 | Cement clinker production capacity across the counties in China in 2020 (a), predicted county-level clinker production of three scenarios (b) and then aggregated to city-level for validation (c). Notes: The reference values of city-level production are from Wang et al., (2024a).

To evaluate the performance of Module 3 in simulating the spatial distribution of clinker production, we applied it to the base year (2020), using observed demand distributions and matching them with existing capacity. Figure 4b shows the county-level clinker production modeled from three demand distribution scenarios (i.e., POP, GDP, and POP-GDP scenarios), relative to their existing production capacities. A noticeable feature is that many points are stacked or overlaid on top of each other, reflecting similar predictions across the scenarios. This indicates

that for most counties, the modeled production values from the different scenarios are relatively consistent. However, a few scattered points highlight differences between the scenarios, where the predicted production capacity varies more significantly across the scenarios. Figure 4c shows the validation of our model results by comparing the predicted production with available city-level clinker production data from Wang et al., (2024a). The R-squared values for the three scenarios are 0.583 (POP), 0.593 (GDP), and 0.608 (POP-GDP), indicating that the combined scenario provides the best fit to the city-level data. The root mean square error (RMSE) values are 3.42 (POP), 3.38 (GDP), and 3.32 (POP-GDP), with the combined scenario again showing the lowest error. This demonstrates the model's relatively good performance in predicting clinker production at the city level.

3.3 Future county-level clinker production and capacity

To meet the future cement demand across China's counties, a number of counties will be required to produce significant amounts of clinker. Figure 5 maps China's county-level clinker production under POP, GDP, and POP-GDP scenarios from 2030 to 2050, with the POP scenarios depicting absolute production (Figure 5a, d, and g) and the GDP (Figure 5b, e, and h) and POP-GDP hybrid (Figure 5c, f, and i) scenarios showing deviations relative to the POP scenario. In 2030, the POP scenario displays the concentrated high production in coastal counties (e.g., Yangtze/Pearl River Deltas), while the GDP scenario amplifies coastal-inland disparities – those counties in Zhejiang and Guangdong Provinces will surge (+2-4 Mt/year) whereas many counties in northern (e.g., Heilongjiang) and western (e.g., Gansu) provinces shall decline. By contrast, the POP-GDP hybrid scenario would harmonize these differences. By 2050, all county-level production will show a significant decrease compared to 2030, due to demographic decline and further saturation of cement stocks in use (Cao et al., 2020, 2017). These trajectories underscore the imperative of capacity adjustment planning should be reconciled with future economic dynamics and demographic change.

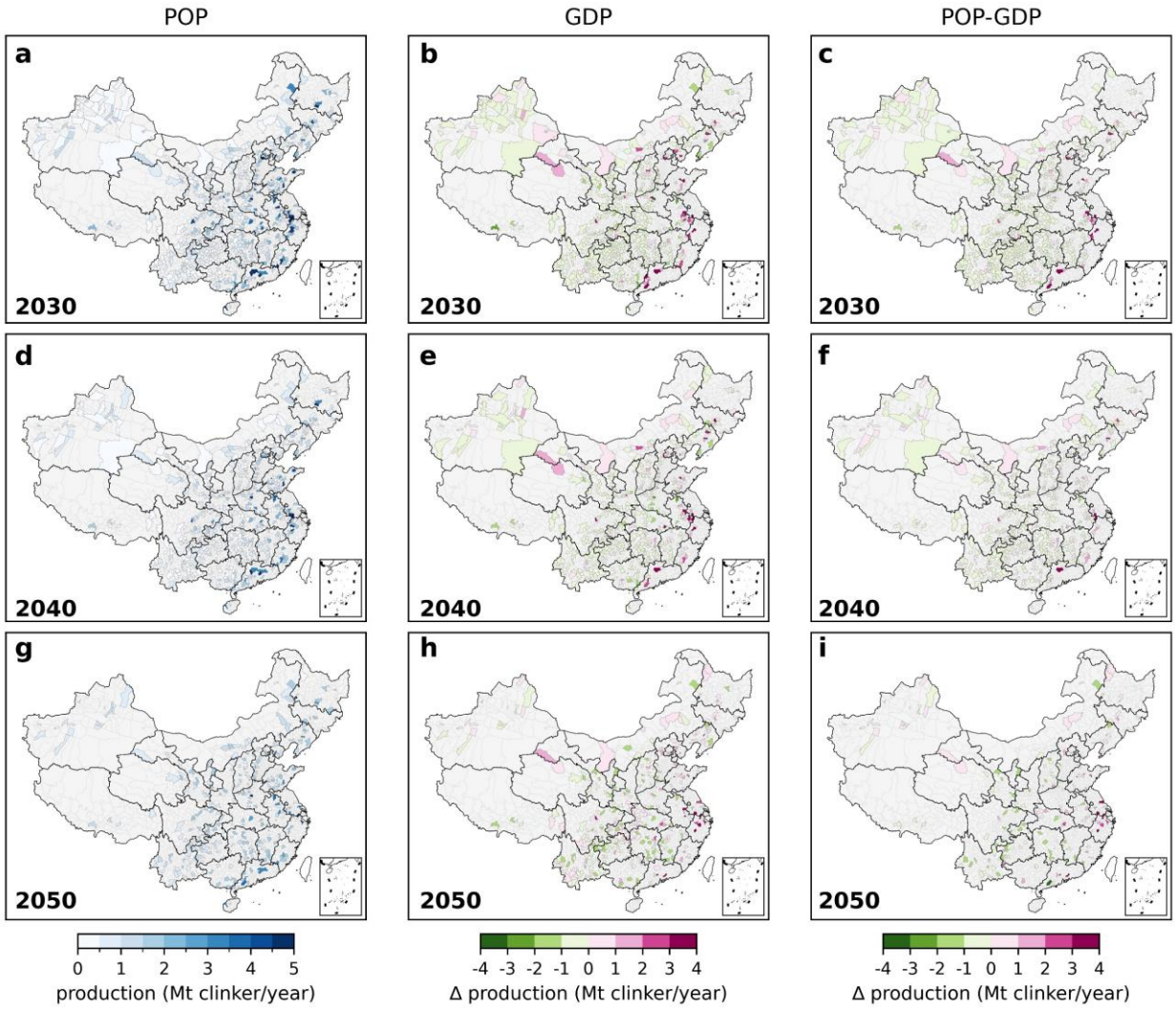

Figure 5 | County-level clinker production of POP scenario in 2030 (a), 2040 (d), and 2050 (g), and the changes of GDP scenario (b, e, and h) and POP-GDP (c, f, and i) scenario compared to the POP scenario.

At the same time, clinker production capacity will vary with future demand. As shown in Figure 6a, the county-level capacities would decrease slightly under the POP scenario compared to the existing capacity in Figure 4a. However, the GDP scenario amplifies the regional disparities again – counties such as Fanchang County in Wuhu City would experience an increase of about 17 Mt/year in capacity, while Baofeng County in Pingdingshan City would see a decrease of around 5Mt/year capacity compared to the POP scenario. These deviations would be moderated under the POP-GDP hybrid scenario. After 2030, all the county-level capacities are expected to shrink further (Figure 6d, e, and f). By 2050, most counties that still have a remaining clinker production capacity of less than 2 Mt/year (Figure 6g). Notably, these patterns underscore the importance of adjusting cement production capacity and planning for CCS deployment in response to the future demographic and economic shifts across different regions.

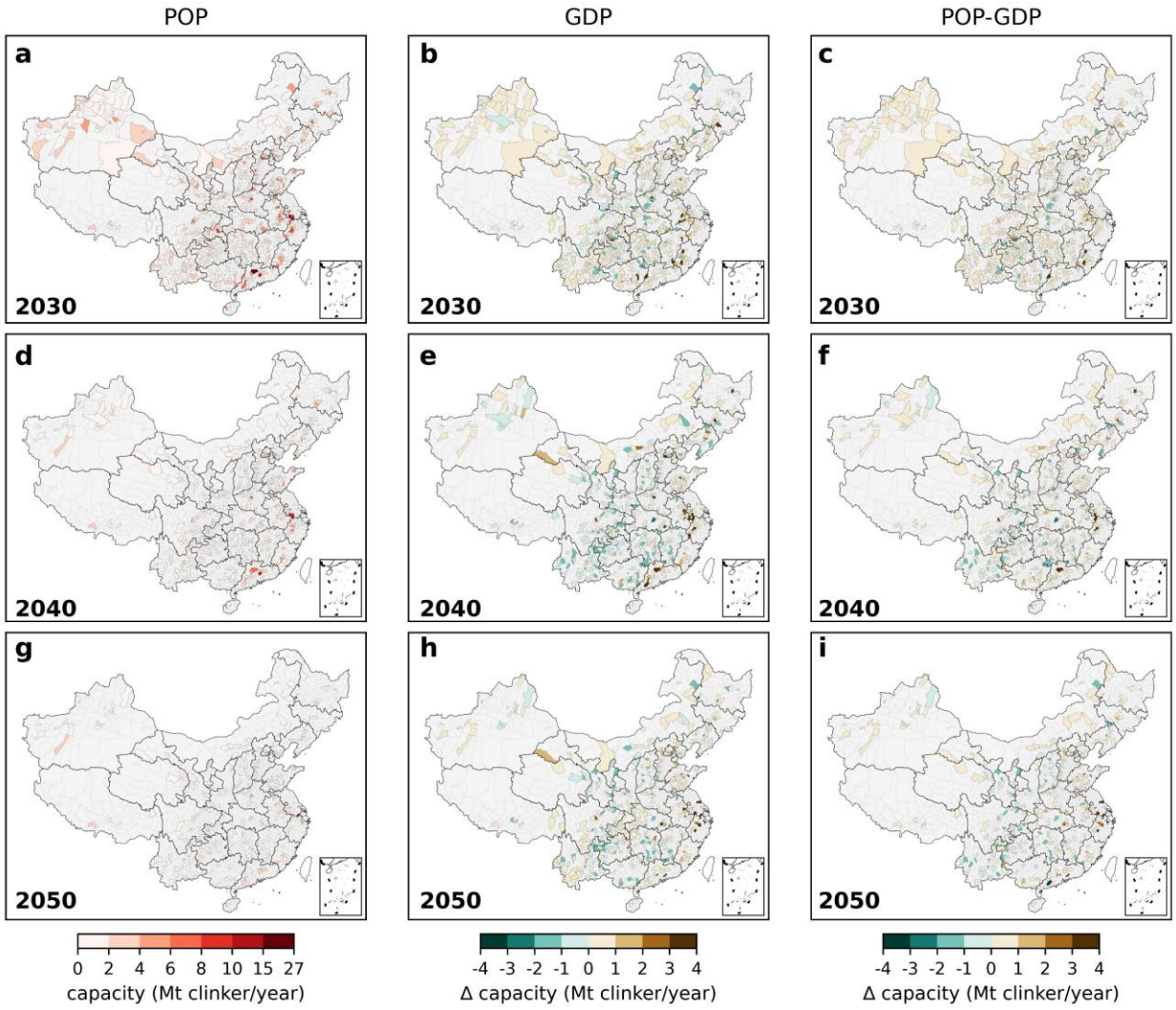

Figure 6 | County-level clinker production capacity of POP scenario in 2030 (a), 2040 (d), and 2050 (g), and the changes of GDP scenario (b, e, and h) and POP-GDP hybrid scenario (c, f, and i) compared to the POP scenario.

3.4 Prioritized counties for CCS deployment

3.4.1 Carbon emissions from future clinker production

As shown in Figure 7, the cumulative carbon emissions from clinker production during 2021–2050 are estimated based on the county-level production and emission factors. Under the POP scenario, emissions are highly concentrated in major production hubs, particularly in eastern and southern China, including the junction of Anhui, Zhejiang, and Jiangsu provinces, as well as northern Guangdong (Figure 7a). Counties in these regions are expected to exhibit emissions exceeding 100 Mt-CO_2, highlighting their significant role in emissions mitigation. For instance, Liyang in Changzhou city would have the highest total emissions, reaching 300 Mt-CO_2. In contrast, under the GDP scenario, most counties experience emission reductions, with these reductions shifting toward and becoming concentrated in developed production hubs (Figure 7b). Notably, cumulative

emissions in Liyang (Changzhou city), Yingde (Qingyuan city), and Fanchang (Wuhu city) will increase by 120, 207, and 263 Mt-CO_2, respectively, compared to the POP scenario. The POP-GDP scenario moderates these shifts by balancing population and economic factors, leading to a more even distribution of emissions changes across counties (Figure 7c). Overall, these spatial patterns of cumulative emissions, shaped by future clinker demand and production layouts, provide an important basis for emissions mitigation strategies and the deployment of low-carbon technologies in high-emission regions.

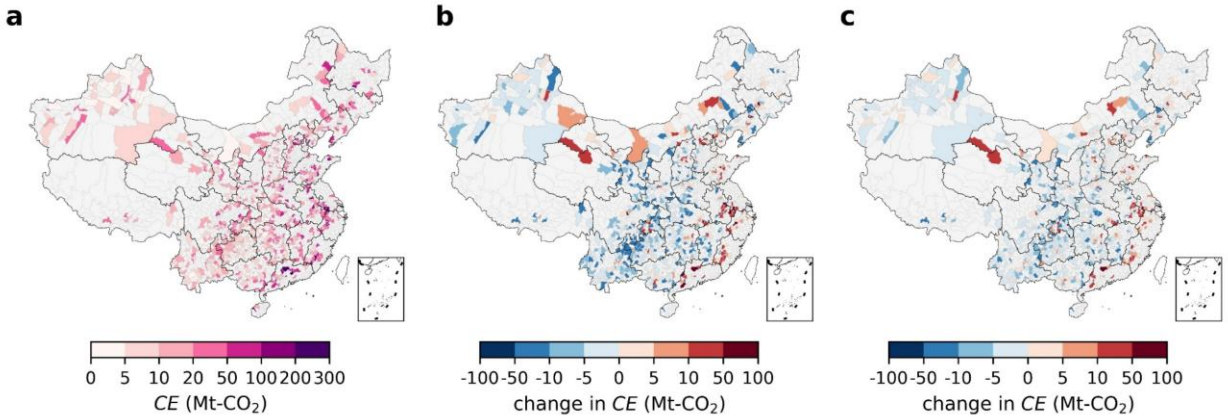

Figure 7 | Cumulative carbon emissions from clinker production during 2021-2050 of POP (a), GDP (b), and POP-GDP (c) scenarios. (Notes: *CE* represents cumulative emissions.)

3.4.2 Carbon storage capacity

The carbon storage potentials of deep saline aquifers (DSA) and CO_2-enhanced oil recovery (CO_2-EOR) across China's counties are depicted in Figure 8 below. There are 1,381 cities exhibiting a storage capacity for DSA, while 92 cities possessing a capacity for CO_2-EOR. Cumulatively, the total storage capacity is estimated at ~85 Gt CO_2 for DSA and ~9.0 Gt CO_2, respectively. The counties in Xinjiang stand out with the largest potential to sequester up to ~23 Gt CO_2 via DSA, primarily due to the presence of large basins such as the Tarim Basin and Junggar Basin (Figure 8a). In contrast, CO_2-EOR storage is more localized, primarily concentrated in the Songliao Basin in Northeast China, the Tarim Basin in Northwest China, and the Bohai Bay Basin in North China, where abundant oil reserves provide opportunities for enhanced oil recovery (Figure 8b). These highlighted regions emerge as key areas for long-term CO_2 sequestration due to their extensive geological formations, making them critical for future carbon capture and storage (CCS) deployment.

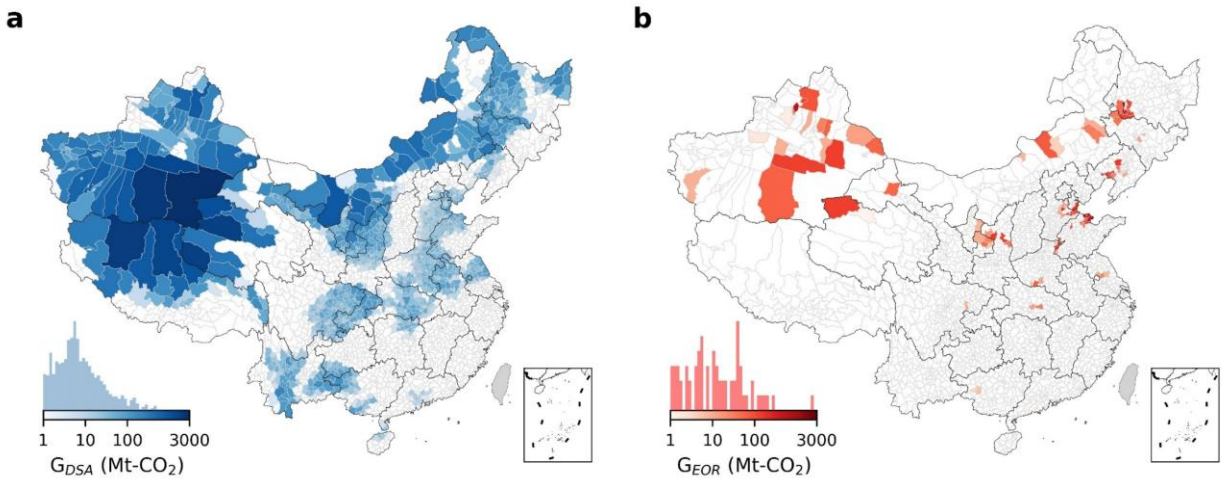

Figure 8 | Carbon storage capacity of deep saline aquifers (a) and enhanced oil recovery (b) across China's counties. (Notes: DSA denotes deep saline aquifers, and EOR represents enhanced oil recovery.)

3.4.3 Matching carbon emissions with storage capacity

After matching the cumulative carbon emissions from clinker production with available storage capacity while minimizing the transportation distances, the stored emissions versus weighted transportation distances (WTD) are displayed for the three scenarios (Figure 9a). The results indicate that most counties have cumulative stored emissions below 100 Mt-CO_2, but with variable WTD patterns, reflecting the spatial differences in storage accessibility. Notably, counties within 300 km WTD store the majority of emissions, benefiting from their proximity to deep saline aquifers and enhanced oil recovery sites, allowing for more efficient carbon sequestration. Between 300 and 500 km WTD, the stored emissions are more dispersed, suggesting that while storage options are still accessible, moderate transport is required. In this range, counties under the GDP scenario are more prevalent, highlighting that economically driven clinker demand shifts emissions toward regions with less immediate storage availability. In contrast, the POP-GDP scenario achieves better clustering, implying that incorporating both economic and demographic considerations helps mitigate excessive transport distances. Counties falling between 500 and 800 km WTD are largely concentrated in high-emission but storage-limited regions, particularly in eastern and southern China, where industrial hubs generate substantial emissions but lack local sequestration sites. The POP-GDP scenario sees fewer cases in this range, reinforcing its balanced allocation strategy.

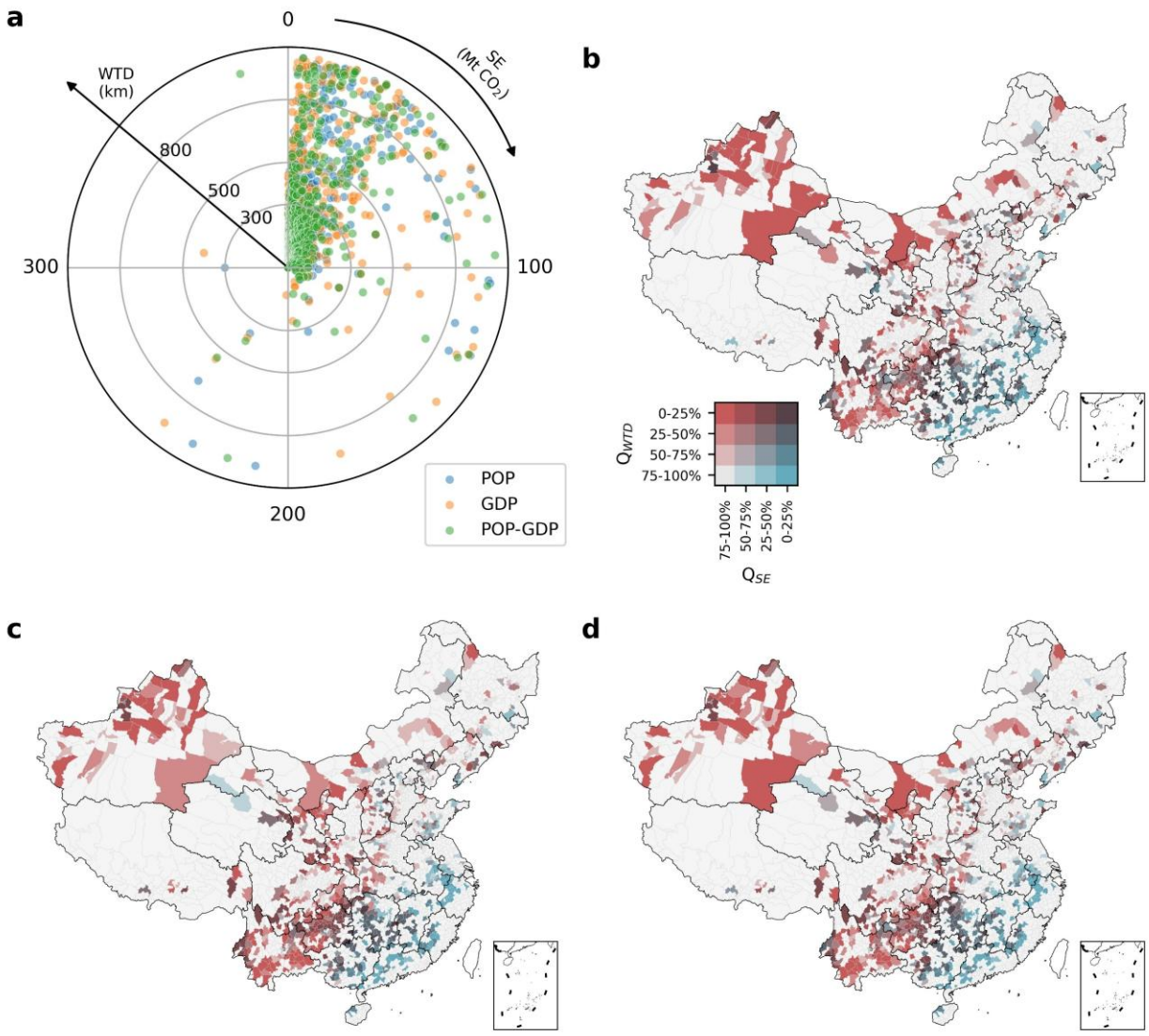

Figure 9 | Emissions-storage matching results (a) and county-level hotspots for POP (b), GDP (c), and POP-GDP (d) scenarios. (Notes: SE represents cumulative captured and stored carbon emissions from clinker production. WTD denotes the weighted transportation distances for stored emissions. WTD quantiles are sorted ascendingly by distance, and stored emissions descendingly by magnitude.)

To identify the counties prioritized for CCS development, Figure 9 (b–d) further illustrate spatial hotspots based on the quantiles of stored cumulative emissions and the WTD required to reach storage sites. Across the three scenarios, 358 counties consistently fall into the same quantile groups, while 453 counties shift their status depending on the scenario. Notably, major production hubs in the eastern and southern coastal regions—including the junction of Zhejiang, Anhui, and Jiangsu provinces, as well as western Fujian and northern Guangdong—are generally assigned a low priority for CCS deployment. This is primarily due to their longer WTD despite their significant emissions scale. For example, although northern Guangdong hosts storage sites with a capacity of approximately 215 Mt-CO_2, these are insufficient to accommodate the region's substantial committed emissions arising from clinker production, which could reach up to 1.6 Gt-

CO_2. In contrast, the western and southwestern regions, such as Yunnan, Guizhou, and Xinjiang, may hold a higher priority due to their shorter WTD and substantial emissions designated for storage. Additionally, some counties exhibit considerable shifts in their priority status across different scenarios due to evolving demand and production layouts. These findings highlight the necessity of optimized spatial CCS deployment to minimize the transportation and pipeline construction costs while ensuring that high-emission regions can effectively access the nearby storage sites.

3.5 Discussions

Most carbon emissions from cement production originate from clinker production. Consequently, regions with higher clinker production should be the primary focus for emission reduction efforts, including the deployment of CCS for a net-zero transition. However, previous studies have rarely planned decarbonization roadmaps in a spatially explicit manner. This study attempts to address this gap by simulating the future clinker demand and production at the county level across three representative demand scenarios developed. Cumulative production emissions are then matched with the available storage sites to identify counties with high priority for CCS deployment. The results are clear, i.e., counties with substantial clinker production and significant carbon storage capacity should be prioritized for CCS deployment in the coming decades. Conversely, cities located far from the storage sites may not be suitable for large-scale deployment, mainly due to potentially high transportation costs. Policy recommendations can, therefore, be formulated accordingly. For instance, the central government should consider developing industrial policies aimed at a gradual retirement of production capacity in low-priority cities. This part of capacity could then be transferred to the high-priority cities, which would better prepare for the future large-scale deployment of CCS. Additionally, such a strategy would help reduce the transportation costs associated with future carbon storage. By concentrating the production capacity and CCS deployment in strategically advantageous locations, the efficiency and effectiveness of overall decarbonization efforts can be significantly enhanced.

There are few limitations in this study. First, there are still some uncertainties in estimating the carbon storage potentials of deep saline aquifers due to several parameters with large uncertainties. Second, the analysis considers only the highway driving distance as a proxy for city distances. Although road transport currently accounts for majority of cement and clinker transportation, the increasing share of railway and waterborne transport introduces potential bias into the results. Third, instead of using the Delaunay triangulation to link all the emission sources and sinks as suggested by Tang et al. (2023), highway driving distance is employed as a distance proxy in emissions-storage matching. This approach not only assumes that part of emissions will be transported by road but also implicitly suggests that CO_2 transportation pipelines will be constructed along the existing highways to overcome the terrain obstacles. Fourth, our model does not incorporate policy-driven scenarios such as carbon taxes or CCS subsidies, due to its simplified representation of cement plants. It cannot yet capture firm-level responses to diverse policy signals.

Future work could adopt agent-based modeling (ABM) to simulate interactions among firms, regulators, and downstream users (Yu et al., 2025).

4. Conclusions

This study provides a spatially explicit assessment of future cement clinker production, its associated carbon emissions, and the potential for carbon capture and storage (CCS) deployment across China's counties. By integrating cement demand projections, clinker production capacity estimates, and storage availability, we identified the key regions where CCS could be prioritized. The results reveal that clinker production and emissions will remain concentrated in the production hubs, located in the eastern and southern coastal regions of China, though the overall production is expected to decline by 2050 due to economic transitions and demographic declines. However, a significant spatial mismatch exists between emission sources and storage potential, as many high-emission counties in eastern and southern China lack sufficient nearby storage capacity, while the western and northern regions possess ample storage but lower emissions. The optimized emissions-storage matching analysis highlights that counties in western and southwestern China, such as Yunnan, Guizhou, and Xinjiang, are better suited for CCS deployment due to their relatively short transportation distances and substantial storage availability. In contrast, coastal regions face logistical challenges due to longer required transport distances, reducing their feasibility for large-scale CCS implementation. These findings underscore the necessity of integrating clinker production with the CCS infrastructure to enhance the decarbonization efforts, reduce transportation costs, and improve sequestration efficiency.

Future research should refine carbon storage estimation by improving the geological assessments of deep saline aquifers and CO_2-enhanced oil recovery potential. Additionally, further investigation is needed to explore the impacts of multi-modal CO_2 transportation networks, including the railway and waterborne options, which could lower the transportation costs and enhance the accessibility to remote storage sites. Policy interventions should aim to facilitate a gradual phase-out of production capacity in low-priority regions while incentivizing CCS deployment in strategically prioritized locations. An integrated approach to decarbonize the cement sector—linking production, emissions, and storage planning—is essential for achieving long-term emissions reductions and supporting the global low-carbon transition.

Acknowledgement

The authors would like to thank the Environment and Ecology Bureau and Research Grants Council of the Government of Hong Kong SAR for financially supporting this project through the Green Tech Fund (Grant No.: GTF202110158) and Strategic Topics Grant (Grant No.: STG5/E-103/24-R) respectively.

Supplementary Data

Supplementary data to this article can be found online at https://doi.org/10.1016/j.jclepro.2025.146375.

Data availability

The code and data generated by this paper are available on https://github.com/tongyuanwu/china-cement-ccs-hotspots.

References

Cao, Z., Myers, R.J., Lupton, R.C., Duan, H., Sacchi, R., Zhou, N., Reed Miller, T., Cullen, J.M., Ge, Q., Liu, G., 2020. The sponge effect and carbon emission mitigation potentials of the global cement cycle. Nat Commun 11, 3777. https://doi.org/10.1038/s41467-020-17583-w

Cao, Z., Shen, L., Løvik, A.N., Müller, D.B., Liu, G., 2017. Elaborating the History of Our Cementing Societies: An in-Use Stock Perspective. Environ. Sci. Technol. 51, 11468–11475. https://doi.org/10.1021/acs.est.7b03077

Dinga, C.D., Wen, Z., 2022. China's green deal: Can China's cement industry achieve carbon neutral emissions by 2060? Renewable and Sustainable Energy Reviews 155, 111931. https://doi.org/10.1016/j.rser.2021.111931

Fennell, P.S., Davis, S.J., Mohammed, A., 2021. Decarbonizing cement production. Joule 5, 1305–1311. https://doi.org/10.1016/j.joule.2021.04.011

Gardarsdottir, S., De Lena, E., Romano, M., Roussanaly, S., Voldsund, M., Pérez-Calvo, J.-F., Berstad, D., Fu, C., Anantharaman, R., Sutter, D., Gazzani, M., Mazzotti, M., Cinti, G., 2019. Comparison of Technologies for CO2 Capture from Cement Production—Part 2: Cost Analysis. Energies 12, 542. https://doi.org/10.3390/en12030542

Gartner, E., Sui, T., 2018. Alternative cement clinkers. Cement and Concrete Research 114, 27–39. https://doi.org/10.1016/j.cemconres.2017.02.002

Gibbins, J., Chalmers, H., 2008. Carbon capture and storage. Energy Policy 36, 4317–4322. https://doi.org/10.1016/j.enpol.2008.09.058

Gurobi Optimization, LLC, 2025. Gurobi Optimizer Reference Manual.

Habert, G., Miller, S.A., John, V.M., Provis, J.L., Favier, A., Horvath, A., Scrivener, K.L., 2020. Environmental impacts and decarbonization strategies in the cement and concrete industries. Nat Rev Earth Environ 1, 559–573. https://doi.org/10.1038/s43017-020-0093-3

International Energy Agency, 2019. Transforming Industry through CCUS.

International Energy Agency, 2016. 20 Years of Carbon Capture and Storage - Accelerating Future Deployment.

Lackey, G., Vasylkivska, V.S., Huerta, N.J., King, S., Dilmore, R.M., 2019. Managing well leakage risks at a geologic carbon storage site with many wells. International Journal of Greenhouse Gas Control 88, 182–194. https://doi.org/10.1016/j.ijggc.2019.06.011

Li G., Lv M., 2002. Atlas of China's Petroliferous Basins (2nd Edition). China Petroleum Industry Press, Beijing, China.

Liu, J., Tong, D., Zheng, Y., Cheng, J., Qin, X., Shi, Q., Yan, L., Lei, Y., Zhang, Q., 2021. Carbon and air pollutant emissions from China's cement industry 1990–2015: trends, evolution of technologies, and drivers. Atmos. Chem. Phys. 21, 1627–1647. https://doi.org/10.5194/acp-21-1627-2021

Liu, J., Zhang, S., Wagner, F., 2018. Exploring the driving forces of energy consumption and environmental pollution in China's cement industry at the provincial level. Journal of Cleaner Production 184, 274–285. https://doi.org/10.1016/j.jclepro.2018.02.277

Middleton, R.S., Bielicki, J.M., 2009. A scalable infrastructure model for carbon capture and storage: SimCCS. Energy Policy 37, 1052–1060. https://doi.org/10.1016/j.enpol.2008.09.049

National Bureau of Statistics of China, 2025. National Data [WWW Document]. URL https://data.stats.gov.cn/english/ (accessed 3.4.24).

National Bureau of Statistics of China, 2021. China Statistical Yearbook 2021 [WWW Document]. URL https://www.stats.gov.cn/sj/ndsj/2021/indexch.htm (accessed 3.4.24).

Persits, F.M., Steinshouer, D.W., Klett, T.R., 2000. World Total Petroleum System Summary Result Data, 2000 World Petroleum Assessment. https://doi.org/10.5066/P9CV5L0E

Ren, M., Ma, T., Fang, C., Liu, X., Guo, C., Zhang, S., Zhou, Z., Zhu, Y., Dai, H., Huang, C., 2023. Negative emission technology is key to decarbonizing China's cement industry. Applied Energy 329, 120254. https://doi.org/10.1016/j.apenergy.2022.120254

Szulczewski, M.L., MacMinn, C.W., Herzog, H.J., Juanes, R., 2012. Lifetime of carbon capture and storage as a climate-change mitigation technology. Proc. Natl. Acad. Sci. U.S.A. 109, 5185–5189. https://doi.org/10.1073/pnas.1115347109

Tan, C., Yu, X., Guan, Y., 2022. A technology-driven pathway to net-zero carbon emissions for China's cement industry. Applied Energy 325, 119804. https://doi.org/10.1016/j.apenergy.2022.119804

Tang, H., Chen, W., Zhang, S., Zhang, Q., 2023. China's multi-sector-shared CCUS networks in a carbon-neutral vision. iScience 26, 106347. https://doi.org/10.1016/j.isci.2023.106347

Tang, H., Zhang, S., Chen, W., 2021. Assessing Representative CCUS Layouts for China's Power Sector toward Carbon Neutrality. Environ. Sci. Technol. 55, 11225–11235. https://doi.org/10.1021/acs.est.1c03401

United States Geological Survey, 1999. Geologic Provinces of the Far East, 2000 (prv3al).

Van Ruijven, B.J., Van Vuuren, D.P., Boskaljon, W., Neelis, M.L., Saygin, D., Patel, M.K., 2016. Long-term model-based projections of energy use and CO2 emissions from the global steel and cement industries. Resources, Conservation and Recycling 112, 15–36. https://doi.org/10.1016/j.resconrec.2016.04.016

Voldsund, M., Gardarsdottir, S., De Lena, E., Pérez-Calvo, J.-F., Jamali, A., Berstad, D., Fu, C., Romano, M., Roussanaly, S., Anantharaman, R., Hoppe, H., Sutter, D., Mazzotti, M., Gazzani, M., Cinti, G., Jordal, K., 2019. Comparison of Technologies for CO2 Capture from Cement Production—Part 1: Technical Evaluation. Energies 12, 559. https://doi.org/10.3390/en12030559

Wang, T., Sun, F., 2022. Global gridded GDP data set consistent with the shared socioeconomic pathways. Sci Data 9, 221. https://doi.org/10.1038/s41597-022-01300-x

Wang, X., Meng, X., Long, Y., 2022. Projecting 1 km-grid population distributions from 2020 to 2100 globally under shared socioeconomic pathways. Sci Data 9, 563. https://doi.org/10.1038/s41597-022-01675-x

Wang, Y., Wen, Z., Xu, M., Chen, J., He, P., 2024a. Plant-level green transformation strategy in China's cement industry: Considering energy conservation and emission reduction co-benefits. Journal of Cleaner Production 467, 142945. https://doi.org/10.1016/j.jclepro.2024.142945

Wang, Y., Wen, Z., Xu, M., Kosajan, V., 2024b. The carbon-energy-water nexus of the carbon capture, utilization, and storage technology deployment schemes: A case study in China's cement industry. Applied Energy 362, 122991. https://doi.org/10.1016/j.apenergy.2024.122991

Wang, Yihan, Xu, M., Lv, X., Wen, Z., Chen, C., 2023. The eco-efficiency evaluation in China's cement industry: A city-level study. Science of The Total Environment 865, 161132. https://doi.org/10.1016/j.scitotenv.2022.161132

Wang, Yu, Yi, H., Tang, X., Wang, Yaxin, An, H., Liu, J., 2023. Historical trend and decarbonization pathway of China's cement industry: A literature review. Science of The Total Environment 891, 164580. https://doi.org/10.1016/j.scitotenv.2023.164580

Watari, T., Cao, Z., Hata, S., Nansai, K., 2022. Efficient use of cement and concrete to reduce reliance on supply-side technologies for net-zero emissions. Nat Commun 13, 4158. https://doi.org/10.1038/s41467-022-31806-2

Wei, Y.-M., Kang, J.-N., Liu, L.-C., Li, Q., Wang, P.-T., Hou, J.-J., Liang, Q.-M., Liao, H., Huang, S.-F., Yu, B., 2021. A proposed global layout of carbon capture and storage in line with a 2 °C climate target. Nat. Clim. Chang. 11, 112–118. https://doi.org/10.1038/s41558-020-00960-0

Wu, T., Ng, S.T., Chen, J., 2025. Incorporating carbon capture and storage in decarbonizing China's cement sector. Renewable and Sustainable Energy Reviews 209, 115098. https://doi.org/10.1016/j.rser.2024.115098

Wu, T., Ng, S.T., Chen, J., 2022. Deciphering the CO<sub>2<sub> emissions and emission intensity of cement sector in China through decomposition analysis. Journal of Cleaner Production 352, 131627. https://doi.org/10.1016/j.jclepro.2022.131627

Wu, T., Ng, S.T., Chen, J., Cao, Z., 2023. More intensive use and lifetime extension can enable net-zero emissions in China's cement cycle. Resources, Conservation and Recycling 198, 107144. https://doi.org/10.1016/j.resconrec.2023.107144

Xu, J., Yang, J., Dong, J., Li, S., Xing, J., Zhao, Y., 2024. An estimation of future county-level cement production and associated air pollutant emissions in China through artificial neural networks. Science of The Total Environment 953, 176036. https://doi.org/10.1016/j.scitotenv.2024.176036

Yu, B., Fu, J., Dai, Y., 2025. Multi-agent simulation of policies driving CCS technology in the cement industry. Energy Policy 199, 114527. https://doi.org/10.1016/j.enpol.2025.114527

Zhang, C.-Y., Yu, B., Chen, J.-M., Wei, Y.-M., 2021. Green transition pathways for cement industry in China. Resources, Conservation and Recycling 166, 105355. https://doi.org/10.1016/j.resconrec.2020.105355

Zhang, S., Worrell, E., Crijns-Graus, W., 2015. Evaluating co-benefits of energy efficiency and air pollution abatement in China's cement industry. Applied Energy 147, 192–213. https://doi.org/10.1016/j.apenergy.2015.02.081